Journal of
Nanoscience and Nanotechnology
Vol. 8, 1–8, 2008

Scratch and Wear Resistance of Polyamide 6 Reinforced with Multiwall Carbon Nanotubes

Luis F. Giraldo[1,2], Witold Brostow[2], Eric Devaux[3], Betty L. López[1,*], and León D. Pérez[1,2]

[1] *Grupo Ciencia de los Materiales, Instituto de Química, Universidad de Antioquia, Calle 62 #52-59 Torre 1 Lab 310, Medellín, Colombia*
[2] *Laboratory of Advanced Polymers and Optimized Materials (LAPOM), Department of Materials Science and Engineering, University of North Texas, Denton, TX 76203-5308, USA*
[3] *Laboratoire de Génie et Matériaux Textiles (GEMTEX), UPRES EA2161, Ecole Nationale Supérieure des Arts et Industries Textiles (ENSAIT), 9, rue de l'Ermitage – BP 30329, 59056 Roubaix Cedex 01, France*

While carbon nanotubes have been used for a variety of purposes, it was not known whether they can improve tribological properties of polymers. Polyamide 6 (PA6) has been reinforced with 0.2, 0.5 and 1.0 wt% of multiwall carbon nanotubes (MWCNTs) by melt mixing process and characterized by scanning electron microscopy (SEM), transmission electron microscopy, thermogravimetric analysis (TGA), scratching, sliding wear and tensile testing. TGA results for the air atmosphere show that MWCNTs shift the onset of thermal degradation to higher temperatures. Sliding wear tests show that the penetration depth decreases as the concentration of carbon nanotubes increases. However, the viscoelastic healing is hampered by the MWCNTs presence and the residual depths increase at the same time. Narrower scratch groove widths are seen in SEM for composites with MWCNTs, and scratch hardness increases. Tensile tests show an increase of 27% in the Young modulus value upon addition of 1.0% of MWCNTs. The stress at yield is also higher for the nanocomposites.

Keywords: Scratch Resistance, Carbon Nanotubes, Polyamide 6, Sliding Wear.

RESEARCH ARTICLE

1. INTRODUCTION

The polymers are replacing metals due to low cost, low density, vibration damping and ease of processing, but their application requires a better understanding and control of their properties. In order to increase the service lifetime of polymeric materials, it is important to improve their tribological and mechanical properties.[1–20] Abrasion and wear typically result in the loss of optical properties needed in clear coats and other uses that require scratch resistance.[5,7,8] In this situation a variety of approaches is used to enhance polymer tribology, including *blending*,[4,6] using *fillers* of various kinds such as carbon black,[21] silica prepared from microemulsions,[19] ceramic fiber mats[12] or metal particles,[22–24] or else *magnetic field imposition*.[25]

Among various tribological techniques, determination of scratch resistance seems to be one of the most important.[6,10] Moreover, a useful measure of wear is obtained in sliding wear—consisting of repetitive scratch testing along the same groove.[11,13,15,17] In most polymers we have observed a limit of the residual depth R_h reached after a certain number of sliding wear tests.[11,13,15] Polystyrene (PS) does not exhibit such a limit, a fact explained by its unusual brittleness.[20]

Among methods of reinforcement of polymeric matrices, we shall focus now on the use of carbon nanotubes (CNTs). CNTs are in use for a variety of purposes, such as creation of fluorescent supramolecular nanoassemblies[26] or reinforcement of aluminum.[27] Actually, other kinds of nanotubes such as made of TiO_2 (Ref. [28]) or boron nitride[29] are also in use. CNTs are known to increase the Young modulus and also electric conductivity of polymers.[30–32]

The need to improve polymer tribology plus enthusiastic literature reports on CNTs have led us to the idea of taking Polyamide 6 (PA6) and reinforcing it with multiwall carbon nanotubes (MWCNTs). Polyamide 6 is a widely used polymer with a tradition.[33] The results are reported below.

2. EXPERIMENTAL DETAILS

2.1. Materials

PA6 was from Aldrich Chemicals Co., Milwaukee, WI. MWCNTs were from Nanocyl, Sambreville, Belgium. The

*Author to whom correspondence should be addressed.

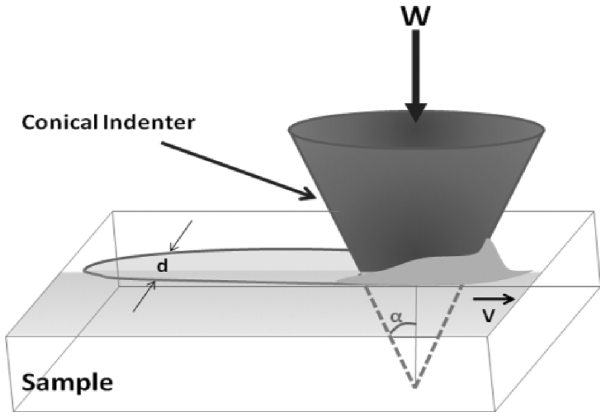

Fig. 1. A schematic of the scratching geometry. α = half angle cone; W = normal load; v = sliding velocity; d = scratch width.

average nanotube diameter is ≈60 nm; it has been determined by transmission electron microscopy, see Section 5 below.

2.2. Scratch Testing

The tests are carried out using a CSM Micro-Scratch Tester (MST), from Neuchatel, Switzerland. Both single scratches and sliding wear (=15 scratches) were performed under the following conditions: normal load 5, 10, 15, 20 and 25 N; scratch length 5 mm; 5 mm/minute scratch speed at the room temperature (24 °C). A conical diamond indenter was used in all the tests with the diameter of 200 μm and the cone angle 120° (Fig. 1). The instantaneous penetration depth R_p and the residual (healing) depth R_h are thus obtained as a function of the number of scratches for a given applied load.

2.3. Microscopy Analysis

JEOL JSM T-300 scanning electron microscope (SEM) was used. The nanocomposites were sputter coated with a thin layer of gold for three minutes in order to induce conductivity in the samples.

The carbon nanotubes were placed in 5 ml of absolute ethanol and sonicated (Bransonic® 1510R-MT, Electron Microscopy Sciences, Washington, PA) for 20 minutes. A drop from of the suspension was placed on a 200-mesh copper grids (Electron Microscopy Sciences, Washington, PA) coated with Formvar. Samples were viewed and photographed using a Zeiss EM 109-T transmission electron microscope (TEM, Carl Zeiss, Inc., Thornwood, NY).

2.4. Nanocomposite Preparation

Several samples of nanocomposites (40 g each) were prepared by melt mixing PA6 and 0.2, 0.5 and 1.0 wt% MWCNTs in a Brabender Preparation Station at 250 °C and at 80 rpm for 10 minutes and then pelletized. A 40 g PA6 sample without filler was used for comparisons.

2.5. Tensile Tests

The tensile tests were carried out using a QTEST5 tensile MTS tensile machine at room temperature (24 °C) with the crosshead speed of 5 mm/minute. The results reported represent each an average of five runs.

Dogbone shape Type IV specimens made according to the ASTM D-638 standard were prepared by compression molding at 250 °C at the pressure of 17.2 MPa. Two Teflon films and two polished stainless steel platens were used. The pellets were placed in the mold and covered with Teflon films and plates. When the plates were in contact with the heated compression molding platen after reaching the desired temperature, they were held at that temperature for 5 minutes. The pressure of 6.9 MPa was applied for 2 minutes, and then the final pressure increased up to 17.2 MPa. In the last step, molded coupons were cooled to room temperature.

2.6. Thermal Analysis

Together with differential scanning calorimetry (DSC), thermogravimetric analysis (TGA) is an established and well described technique.[34–37] The thermogravimetric analysis (TGA) was performed in a Q500 machine from TA Instruments. The nanocomposites were heated up to 800 °C at 10 K/minute in the air atmosphere.

3. THERMAL STABILITY

As noted in the beginning of this article, there is an on going process of replacement of metallic components and structures by polymeric ones. However, metals have temperature service ranges extending far higher than polymer-based materials (PBMs).[1, 38] Therefore, we have decided to find out whether MWCNTs can extend the service temperature range of Polyamide 6 upwards.

Figure 2 shows the TGA results obtained as explained in Section 2 for pure MWCNTs.

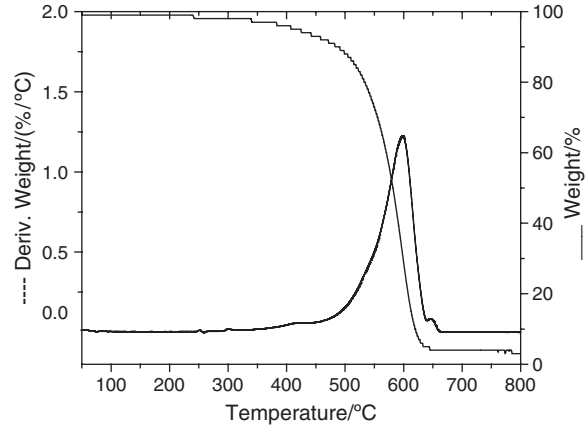

Fig. 2. Thermogravimetric analysis results for multiwall carbon nanotubes.

RESEARCH ARTICLE

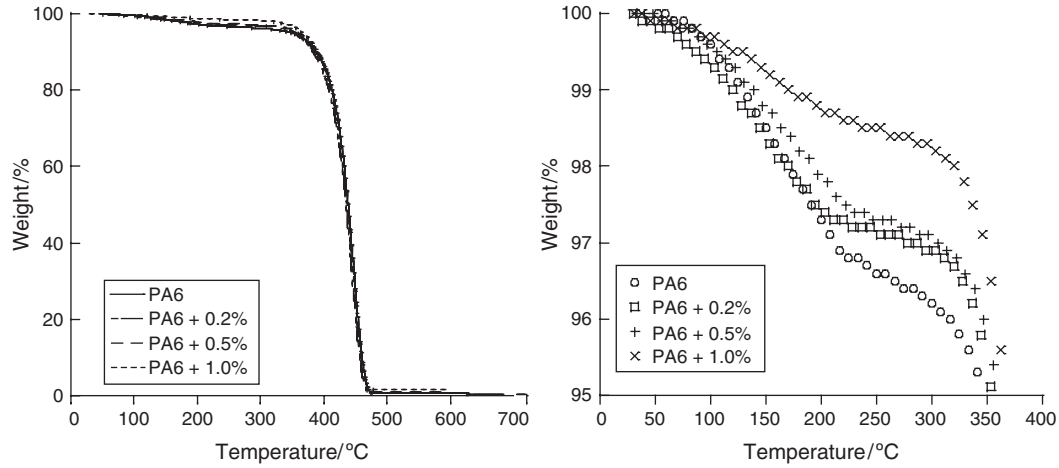

Fig. 3. Thermogravimetric analysis of PA6 nanocomposites. Left: full scale; right: a magnified region.

At 350 °C only 5% of the sample had been decomposed—what corresponds to amorphous carbon.[39–42] According to the derivative curve, the main weight loss occurs around 600 °C—what corresponds to MWCNTs. The purity of the sample is 96% since the metal residue is only 4%. This suggests the existence of an homogeneous material, a conclusion confirmed by mean of a morphological characterization in Section 5.

In Figure 3 left we see that the precipitous drop of weight above 400 °C is similar for all compositions. Figure 3 right tells us that in the oxidizing (air) atmosphere the MWCNTs strengthen the material against thermal degradation. The beginning of the degradation is delayed significantly, particularly so for 1.0 wt% MWCNTs. We recall the explanation of Gilman:[43] thermal degradation is easier when molecules have higher mobility at the interface. Apparently the presence of MWCNTs lowers the mobility, and thus improves the thermal stability of PA6. Nanosize silica particles cause a similar effect, as found in TGA investigation of poly(methyl acrylate) + mesoporous silica nanohybrids.[44]

4. SLIDING WEAR

Viscoelastic materials exhibit a *healing* process: after 3 minutes or so after being "attacked" by the indenter, the bottom of the groove goes up significantly.[6, 10] We wait 5 minutes until we determine the residual or healing depth R_h. This is even better seen in molecular dynamics computer simulations[16, 45] which provide a continuous dependence of the scratch depth of each surface segment on time $R(t)$ rather than just two averages.

For brevity we do not include here results of single scratch experiments. Figure 4 shows the sliding wear behavior in terms of R_p and R_h for our nanocomposites. The definition of sliding wear W we use has been provided in Ref. [11]:

$$W(F) = \lim_{n\to\infty} R_h(F) \tag{1}$$

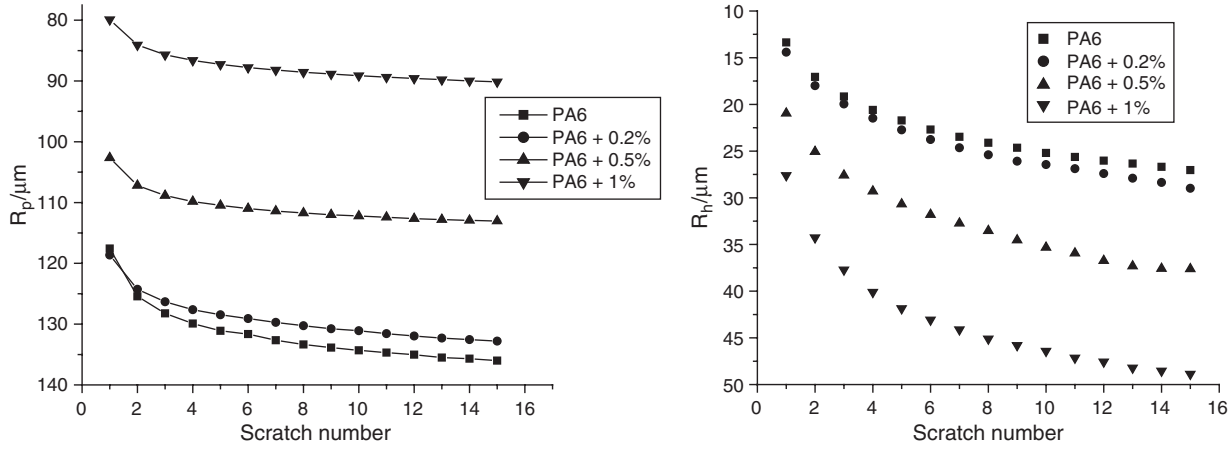

Fig. 4. Multiple scratch behavior of PA6 reinforced with 0.2, 0.5 and 1.0 wt% WCNTs at the constant load of 15.0 N. Left: Instantaneous penetration depth, right: residual depth.

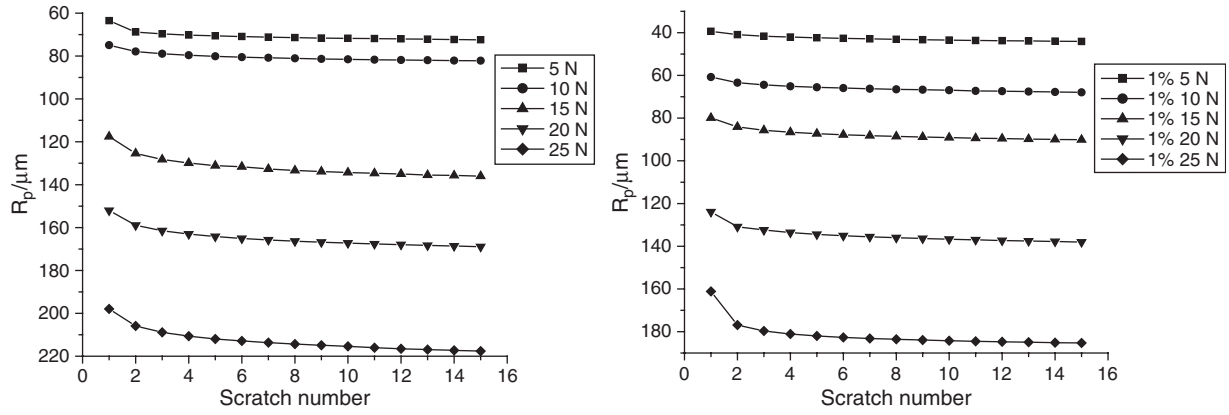

Fig. 5. Penetration depth in sliding wear determination for PA6 and PA6 + 1.0 wt% MWCNTs at several applied loads.

Here F is the load applied while n is the number of scratch tests; we find that usually $n = 15$ is sufficient.[11, 13, 15] Definition (1) is different from the classical and very widely used definition of wear as the mass or volume loss caused by the moving indenter. One reason for Eq. (1) is that accurate determination of the volume or weight loss is quite difficult.

In the left side of Figure 4 we see that the penetration depth *decreases* when increasing the carbon nanotubes concentration. Already at 0.2 wt% of nanotubes filler there is a visible reduction in the R_p. For the 0.2 and 0.5 wt% of the filler, the R_p reduction after 15 scratches amounts to 2.4 and 16.9% respectively. A reduction of 33.8% in the penetration depth for the 15th scratch is obtained at 1.0 wt% MWCNTs (136.1 μm for neat PA6 while only 90.1 μm for the composite).

The residual (recovery) depth results in the right side of Figure 4 show a different kind of behavior. Here gradual addition of MWCNTs *increases* the healing depth R_h. We recall the discussion above of the TGA results: the presence of MWCNTs decreases the mobility of polymer chains. This apparently causes two effects. The more MWCNTs we have, the more the composite resists the original indenter attack, hence lower R_p values. However, the more MWCNTs we have, the less the material can recover after scratching, hence higher R_h values. This behavior might be related to the high aspect ratio of the nanotubes. MWCNTs as hollow nanofibers can act not only as reinforcement agent causing steric hindrance to the indenter penetration but also relatively long nanotubes can induce more nucleating sites. Transcrystallization phenomena can occur such as have been reported for polymers reinforced with fibers.[46, 47] Using spherical nanofiller particles, one would expect that the filler would reinforce the material while affecting the chain mobility less. Then both R_p and R_h would be shallower upon the filler addition.

While the nanotubes concentration is an important variable, of comparable importance for wear evaluation is the load imposed by the indenter on the surface. We have investigated this effect also. In the left part of Figure 5 we display the penetration depths at several applied loads for neat PA6. Naturally, higher loads create deeper grooves.

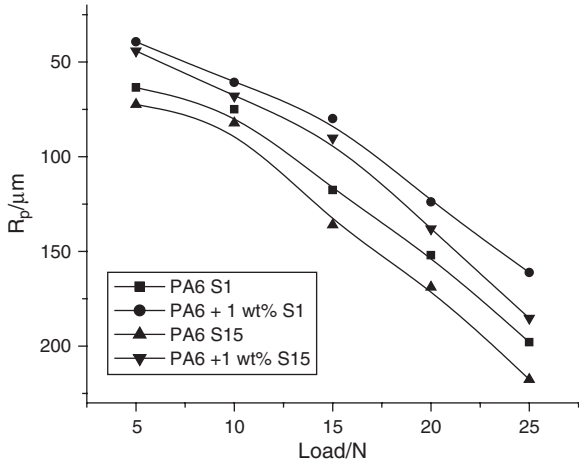

Fig. 6. R_p values for PA6 and for PA6 + 1.0 wt% MWCNTs for the first scratch (S_1) and the fifteenth scratch (S_{15}) as a function of the applied load.

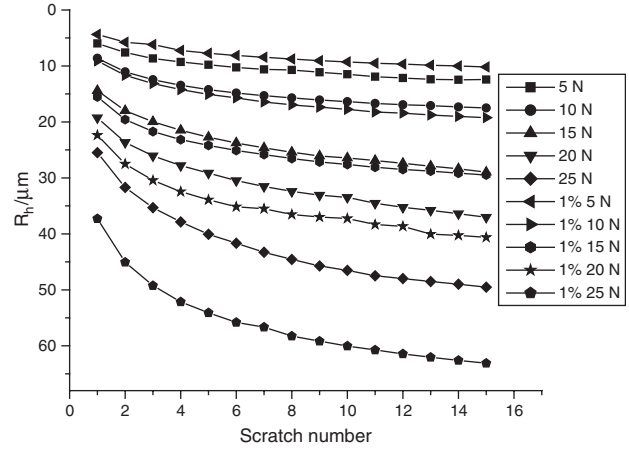

Fig. 7. Residual depth versus the scratch number at several loads for PA6 and PA6 + 1.0% MWCNT.

RESEARCH ARTICLE

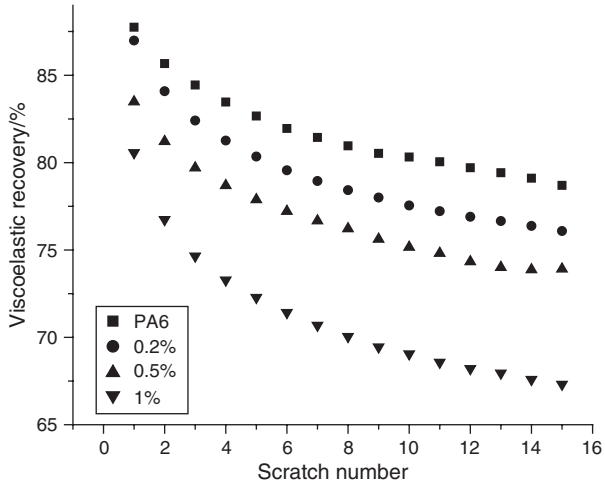

Fig. 8. Viscoelastic recovery (Eq. (2)) of PA6 nanocomposites reinforced with 0.2, 0.5 and 1.0 wt% MWCNTs under the constant load of 15.0 N.

In the right hand side of the same Figure 5 we present similar results for 1.0 wt% MWCNTs.

Comparing both sides of the Figure 5, we see a reduction of R_p caused by the presence of MWCNTs for all applied loads.

The reduction in R_p for different applied loads is considered in a different way in Figure 6. We show R_p values for neat PA6 and for the nanocomposite with 1.0 wt% MWCNTs for single scratch test results and also at the end of the sliding wear tests (15th scratch). As expected from previous diagrams, in the composite a part of the stress imposed by the nanoidenter has been taken up by the nanotubes so that shallower depths result.

In analogy with Figure 5, in Figure 7 we display residual depths R_h as a function of the scratch number and of the applied load for neat PA6 and for PA6 + 1.0 wt% MWCNTs. All samples show an asymptotic behavior of the residual depth with scratch number for the different loads. This is another confirmation of strain hardening in sliding wear in polymers discovered originally in 2004 (Ref. [11]) and seen since in most polymers. Again, the residual depth values are larger for the PA6 reinforced with MWCNTs than for the neat polymer. Thus, the MWCNTs addition seems to be a two-edged sword.

To see better the reason for deeper residual depths, consider now the extent of viscoelastic recovery. The effect can be quantified,[6] namely

$$\phi = (1 - R_h/R_p)100\% \quad (2)$$

The recovery is higher for the first scratches than for later ones. This can be seen in Figure 8. ϕ as defined by Eq. (2) has been connected to brittleness;[20] brittleness has been defined since this term has been used before as a qualitative concept only.[48, 49]

The phenomenon of decreasing viscoelastic recovery with increasing number of scratches can be explained by the *gradual densification* process caused by the consecutive scratches along the same groove.[50] As seen in Figures above, the densification results in strain hardening and the establishment of horizontal asymptotes in the curves of $R_h(n)$; see again Eq. (1).

Figure 8 confirms also the results seen above, namely the fact that the MWCNTs addition results in higher residual depths. The presence of relatively rigid MWCNTs *hampers* the viscoelastic recovery.

5. MORPHOLOGY

We shall now consider possible morphology—properties connections. In Figure 9 (left) we show a SEM micrograph of the MWCNTs. One sees an entangled spaghetti-like structure. The average diameter of a nanotube of ≈60 nm can be seen in the TEM image on the right.

Figures 10 and 11 show the SEM micrographs of the PA6 surfaces without and with MWCNTs, after 15 sliding

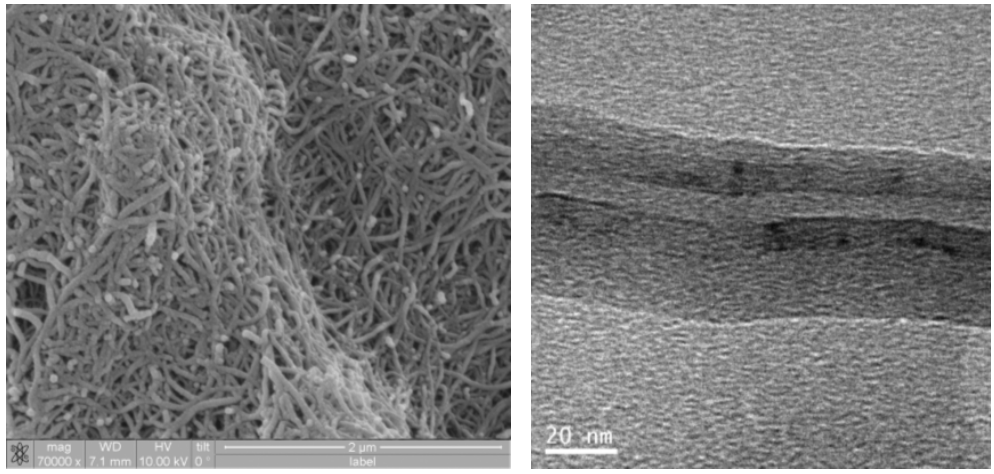

Fig. 9. Left: scanning electron microscopy of MWCNTs. Right: transition electron microscopy of MWCNTs.

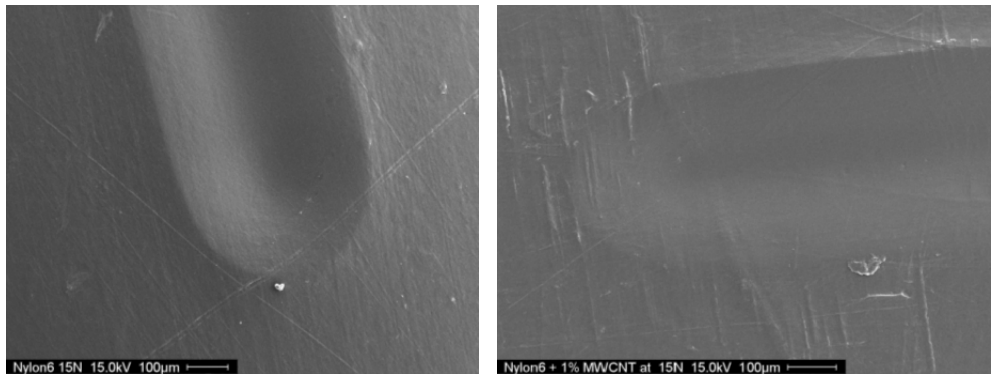

Fig. 10. SEM micrograph of the surface of PA6 (left) and PA6 + 1.0% MWCNTs (right) under 15.0 N after sliding wear (15 times) testing.

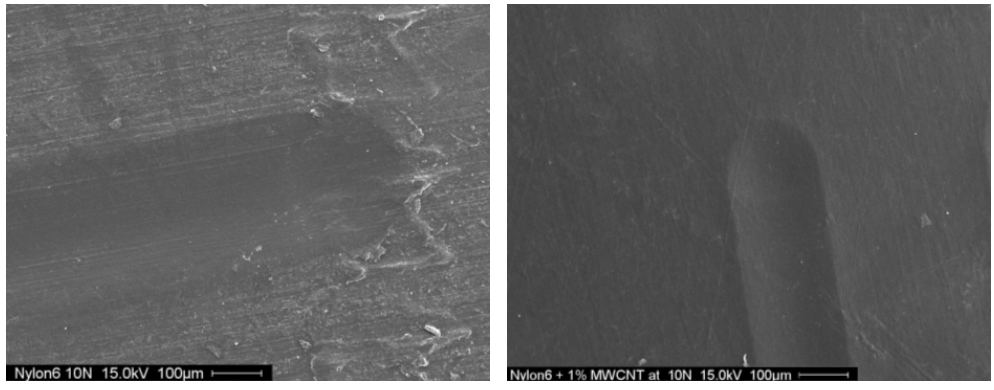

Fig. 11. SEMicrograph of the surface of PA6 (left) and PA6 + 1.0% MWCNTs (right) under 10.0 N after sliding wear (15 times) testing.

wear runs for 15.0 and 10.0 N respectively. Thus, we can see damage on the surfaces; as expected, there is more damage for the higher load. Neat PA6 undergoes a relatively soft deformation. While the addition of MWCNTs increases stiffness, there is no evidence of debris formation on the surface caused by the MWCNTs presence. The SEM images show that for both applied loads (10 and 15 N) there are no flaws or microcracks in the grooves. We observe that the scratch track is wider for PA6 without a filler, CNTs "defend" better the material against the indenter. Neat PA6 shows more plastic deformation that the reinforced samples. This type of behavior with humps at the edges is typical for attack angles between 90°–120°.[51]

6. SCRATCH HARDNESS

There is a belief that hardness is related to scratch behavior; indentation and scratching should be connected.[52] While there are a variety of distinct experiments to determine hardness, the argument is plausible: a softer material would exhibit a larger scratch groove. A relation obtained by Briscoe[51] and used by others[14, 53] for the scratch hardness H_s is

$$H_s = 4P/\pi d^2 \tag{3}$$

Here P is the normal load in N and d is the scratch width determined from the SEM micrographs. Table I summarizes the sliding wear results after 15 indenter passes for 10.0 and 15.0 N loads.

As we see in Table I, the scratch hardness increases significantly upon introduction of the MWCNTs reinforcement. The effect is much larger at the *lower* applied load. These results are apparently related to the loss of viscoelastic recovery calculated above from Eq. (2).

Table I. Scratch hardness.

Sample	P/N	d/μm	H_s
PA6	15	450	94
PA6 + 1.0% MWCNTs	15	400	119
PA6	10	300	141
PA6 + 1.0% MWCNTs	10	200	318

7. TENSILE TESTING

The tensile testing results are summarized in Table II. Each value listed is an average of at least five runs. We can follow effects of introduction of MWCNTs and varying their concentration. Above 0.2 wt% CNTs there is a significant increase of the stress at break.

We see in Table II that again the MWCNTs addition is a two-edged sword. The tensile modulus E goes symbatically with the MWCNTs concentration, as does the

Table II. Tensile testing results.

Sample	Modulus E/MPa	Elong ation to break ε_b/mm	Stress at break σ_b/MPa	% Modulus increase
PA6	1957	1.52	1.11	0
PA6 + 0.2% MWCNTs	2106	1.39	1.10	7.6%
PA6 + 0.5% MWCNTs	2250	1.07	1.76	15.0%
PA6 + 1.0% MWCNT	2482	1.05	2.01	26.8%

stress at break σ_b. However, the elongation at break ε_b decreases at the same time. Unless the storage modulus E' determined in dynamic mechanical testing changes significantly, the ε_b decrease means that the *brittleness*[20] *increases* upon addition of more MWCNTs. Meincke[30] has similarly reported that a loss of PA6 flexibity results in lower ε_b values. Also the results in Table II can be connected to the loss of viscoelastic healing in sliding wear determination seen above in Figure 8.

8. CONCLUDING REMARKS

One large volume application of PA6 is in textile fibers. When good abrasion resistance of textile fibers of PA6 is required, it is worthwhile to reinforce them with a filler such as carbon nanotubes (we do not discuss here the economic consequences of such as an action at the present time). The scratch hardness would increase while avoiding the damage on the surface, without presence of any debris in broad range of applied loads; see again Figures 10 and 11. A good transfer of stress from the filler to the polymeric matrix would take place.

Acknowledgments: We are grateful for financial support to: Ecos Nord Program, Paris; ENSAIT, Roubaix; COLCIENCIAS, Bogotá (*Apoyo a la comunidad científica nacional através de doctorados nacionales 2004*); Robert A. Welch Foundation, Houston (Grant B-1203); and the Universidad de Antioquia, Medellín. Comments of a referee have resulted in improved perspicuity of the present paper.

References and Notes

1. A. Y. Goldman, Prediction of the Deformation Properties of Polymeric and Composite Materials, American Chemical Society, Washington, DC (**1994**).
2. B. J. Briscoe, P. D. Evans, E. Pelillo, and S. K. Sinha, *Wear* 200, 137 (**1996**).
3. V. Jardret, H. Zahouani, J. L. Loubet, and T. G. Mathia, *Wear* 218, 8 (**1998**).
4. W. Brostow, P. E. Cassidy, H. E. Hagg, M. Jaklewicz, and P. E. Montemartini, *Polymer* 42, 7971 (**2001**).
5. J. J. Rajesh, J. Bijwe, U. S. Tewari, and B. Venkataraman, *Wear* 249, 702 (**2001**).
6. W. Brostow, B. Bujard, P. E. Cassidy, H. E. Hagg, and P. E. Montemartini, *Mater. Res. Innovat.* 6, 7 (**2001**).
7. J. Karger-Kocsis and D. Felhös, Friction and Sliding Wear of Nanomodified Rubbers and Their Coatings: Some New Developments in Tribology of Polymeric Nanocomposites, edited by K. Friedrich and A. K. Schlarb, Elsevier, Amsterdam (**2007**).
8. S. Ducret, C. P. Mattéi, V. Jardret, R. Vargiolu, and H. Zahouani, *Wear* 255, 1093 (**2003**).
9. Z. Roslaniec, G. Broza, and K. Schulte, *Compos. Interfaces* 10, 95 (**2003**).
10. W. Brostow, J.-L. Deborde, M. Jaklewicz, and P. Olszynski, *J. Mater. Ed.* 24, 119 (**2003**).
11. W. Brostow, G. Darmarla, J. Howe, and D. Pietkiewicz, *e-Polymers* 025 (**2004**).
12. J. S. Sabo, J. Karger-Kocsis, O. Gryshchuk, and T. Czigany, *Compos. Sci. Tech.* 64, 1717 (**2004**).
13. M. D. Bermúdez, W. Brostow, F. J. Carrión-Vilches, J. J. Cervantes, and D. Pietkiewicz, *e-Polymers* 01 (**2005**).
14. J. J. Rajesh and J. Bijwe, *Wear* 259, 661 (**2005**).
15. M. D. Bermúdez, W. Brostow, F. J. Carrion-Vilches, J. J. Cervantes, G. Damarla, and J. M. Perez, *e-Polymers* 03 (**2005**).
16. W. Brostow and R. Simões, *J. Mater. Ed.* 27, 19 (**2005**).
17. M. D. Bermúdez, W. Brostow, F. J. Carrion-Vilches, J. J. Cervantes, and D. Pietkiewicz, *Polymer* 46, 347 (**2005**).
18. K. Maeda, A. Bismarck, and B. J. Briscoe, *Wear* 259, 651 (**2005**).
19. R. Palkovits, H. Althues, A. Rumplecker, B. Tesche, A. Dreier, U. Holle, G. Fink, C. H. Cheng, D. F. Shantz, and S. Kaskel, *Langmuir* 21, 6048 (**2005**).
20. W. Brostow, H. E. Hagg Lobland, and M. Narkis, *J. Mater. Res.* 21, 2422 (**2006**).
21. W. Brostow, M. Keselman, I. Mironi-Harpaz, M. Narkis, and R. Peirce, *Polymer* 46, 5058 (**2005**).
22. K. Ghosh, *J. Appl. Polym. Sci.* 60, 323 (**1996**).
23. W. Brostow, B. P. Gorman, and O. Olea-Mejia, *Mater. Letters* 61, 1333 (**2007**).
24. W. Brostow, A. Buchman, E. Buchman, and O. Olea-Mejia, in preparation.
25. W. Brostow and M. Jaklewicz, *J. Mater. Res.* 19, 1038 (**2004**).
26. M. Bottini, F. Cerignoli, L. Tautz, N. Rosato, A. Bergamaschi, and T. Mustelin, *J. Nanosci. Nanotechnol.* 6, 3693 (**2006**).
27. T. Laha, Y. Liu, and A. Agarval, *J. Nanosci. Nanotechnol.* 7, 515 (**2007**).
28. Y. Jia, A. Kleinhammes, H. Kulkarni, K. McGuire, L. E. McNeil, and Y. Wu, *J. Nanosci. Nanotechnol.* 7, 458 (**2007**).
29. C. Zhi, Y. Bando, G. Shen, C. Tang, and D. Goldberg, *J. Nanosci. Nanotechnol.* 7, 530 (**2007**).
30. O. Meincke, D. Kaempfer, H. Weickmann, C. Friedrich, M. Vathauer, and H. Warth, *Polymer* 45, 739 (**2004**).
31. H. Miyagawa and L. T. Drzal, *Polymer* 45, 5163 (**2004**).
32. M. Cadek, J. N. Coleman, K. P. Ryan, V. Nicolosi, G. Bister, A. Fonseca, J. B. Nagy, K. Szostak, F. Béguin, and W. J. Blau, *Nano Letters* 4, 353 (**2004**).
33. L. Mathias, R. Vaidya, and J. B. Canterberry, *J. Mater. Ed.* 6, 207 (**1984**).
34. E. M. Pearce, C. E. Wright, and B. K. Bordoloi, *J. Mater. Ed.* 4, 193 (**1982**).
35. E. M. Pearce, C. E. Wright, and B. K. Bordoloi, *J. Mater. Ed.* 4, 345 (**1982**).
36. K. P. Menard, Performance of Plastics, edited by W. Brostow, Hanser, Munich–Cincinnati (**2000**), Chap. 8.
37. B. Bilyeu, W. Brostow, and K. P. Menard, *J. Mater. Ed.* 22, 107 (**2000**).
38. W. Brostow (ed.), Performance of Plastics, Hanser, Munich–Cincinnati (**2000**).

39. X. H. Chen, C. S. Chen, Q. Chen, F. Q. Cheng, G. Zhang, and Z. Z. Chen, *Mater. Letters* 57, 734 **(2002)**.
40. J. Li and Y. Zhang, *Physica E* 28, 309 **(2005)**.
41. J. Moon, K. An, Y. Lee, Y. Park, D. Bae, and G. Park, *J. Phys. Chem. B* 105, 5677 **(2001)**.
42. I. W. Chiang, B. E. Brinson, R. E. Smalley, J. L. Margrave, and R. H. Hauge, *J. Phys. Chem. B* 105, 1157 **(2001)**.
43. J. W. Gilman, *Appl. Clay Sci.* 15, 31 **(1999)**.
44. L. D. Perez, L. F. Giraldo, W. Brostow, and B. L. Lopez, *e-Polymers* 29, 1 **(2007)**.
45. W. Brostow, J. A. Hinze, and R. Simões, *J. Mater. Res.* 19, 851 **(2004)**.
46. J. Varga and J. Karger-Kocsis, *Polym. Commun.* 36, 4877 **(1995)**.
47. H. Shi, Y. Zhao, X. Dong, C. He, D. Wang, and D. Xu, *Polym. Int.* 53, 1672 **(2004)**.
48. E. Werwa, *J. Mater. Ed.* 22, 18 **(2000)**.
49. H. E. Hagg Lobland, *J. Mater. Ed.* 27, 29 **(2005)**.
50. W. Brostow, W. Chonkaew, L. Rapoport, Y. Soifer, and A. Verdyan, *J. Mater. Res.* 22 **(2007)**, in press.
51. B. J. Briscoe, *Tribol. Internat.* 31, 121 **(1998)**.
52. K. Rau, R. Singh, and E. Goldberg, *Mater. Res. Innovat.* 5, 151 **(2002)**.
53. C. Gauthier, S. Lafaye, and R. Schirrer, *Tribol. Internat.* 34, 469 **(2001)**.

Received: 7 February 2007. Revised/Accepted: 10 July 2007.